

# Linear programming-based solution methods for constrained POMDPs

Can Kavaklioglu · Robert Helmechi ·  
Mucahit Cevik

Received: date / Accepted: date

**Abstract** Constrained partially observable Markov decision processes (CPOMDPs) have been used to model various real-world phenomena. However, they are notoriously difficult to solve to optimality, and there exist only a few approximation methods for obtaining high-quality solutions. In this study, we use grid-based approximations in combination with linear programming (LP) models to generate approximate policies for CPOMDPs. We consider five CPOMDP problem instances and conduct a detailed numerical study of both their finite and infinite horizon formulations. We first establish the quality of the approximate unconstrained POMDP policies through a comparative analysis with exact solution methods. We then show the performance of the LP-based CPOMDP solution approaches for varying budget levels (i.e., cost limits) for different problem instances. Finally, we show the flexibility of LP-based approaches by applying deterministic policy constraints, and investigate the impact that these constraints have on collected rewards and CPU run time. Our analysis demonstrates that LP models can effectively generate approximate policies for both finite and infinite horizon problems, while providing the flexibility to incorporate various additional constraints into the underlying model.

**Keywords** Constrained POMDPs, linear programming, integer programming, approximation methods

---

Can Kavaklioglu  
Toronto Metropolitan University, Toronto, Canada

Robert Helmechi  
Toronto Metropolitan University, Toronto, Canada

Mucahit Cevik  
Toronto Metropolitan University, Toronto, Canada  
E-mail: mcevik@ryerson.ca

## 1 Introduction

Markov decision processes (MDPs) model sequential decisions over a finite or infinite number of discrete time intervals, known as decision epochs. In MDPs, the system state is fully observable, but there is uncertainty associated with the state transitions. Specifically, the effects of actions/decisions on the current state are characterised by the transition probability values. As the system state changes and actions are taken, some transitions accrue rewards according to a reward mechanism. Solving an MDP problem constitutes determining an optimal policy, which defines the actions for all states of the process. Because of the relatively simple model structure, it is possible to solve large MDP models (e.g., number of states in the order of tens of thousands) using dynamic programming methods. For even larger problem instances, reinforcement learning strategies have been successfully employed to generate approximate policies.

Not all problems consist of fully observable state spaces. In many real-world problems, directly observing the current system state is not possible. For instance, sensor noise in robotics or inconclusive diagnostic tests in health care problems contribute to ambiguities about the true state of the process. Partially observable MDPs (POMDPs) extend the MDP framework with a set of observations and observation probabilities that provide informative signals about the underlying system state. POMDP models are used in a wide range of applications such as finding victims using UAV images (Bravo et al., 2019), spoken dialogue systems (Young et al., 2013) and the robotic manipulation of objects (Pajarinen and Kyrki, 2017).

Often the real world environments that are modelled by using MDPs involve trade-offs between the expected value and the cost. While these two quantities can be amalgamated into a single reward function, e.g., by using cost definitions as negative terms and value definitions as positive terms, a more rigorous way to model these quantities is to make use of constrained POMDP (CPOMDP) models. CPOMDPs extend POMDPs with constraints that can be defined distinctly from rewards. CPOMDP inference methods take constraint definitions into consideration when identifying optimal policies, which allows us to generate policies that can conform to resource limitations. Typically, CPOMDPs extend POMDP definitions with a cost function, which specifies the amount of resources required to take a particular action in a given state at a given time; and a budget term, which stipulates the total amount of available resources throughout the decision process. The budget term specifies an upper limit for the expected total cost incurred by the policy.

There are numerous examples from the recent literature that use CPOMDPs to find viable solutions to underlying decision problems while obeying the specific problem constraints. These examples include robotic planning (Wang et al., 2015), radar resource management (Schöpe et al., 2021), wireless communication systems (Cui et al., 2013) and disease screening (Cevik et al., 2018). In this study, we adopt grid-based approximations for CPOMDPs and formulate linear programming (LP) models to incorporate various constraints into the decision process. The contributions of our study can be summarized as follows:

- We formulate LP models to generate approximate policies for both finite and infinite horizon CPOMDPs. Specifically, we employ grid-based approximations,

and characterize the transition probabilities between the grid points using an iterative approach.

- We create five CPOMDP instances based on popular unconstrained POMDP test problems from the literature. We conduct a detailed numerical study with these instances and compare our methods with Poupart et al. (2015)’s constraint-based approximate linear programming (CALP) algorithm for CPOMDPs. Accordingly, our analysis sheds light into the effectiveness of approximate solution methods for CPOMDPs.
- We design a simulation mechanism to test the performance of the CPOMDP policies. We report the average collected rewards along with the level of adherence to budget limits. The simulation results show that grid-based approximations can lead to a certain degree of violation of the constraints in some problem instances, which is consistent with the findings of previous studies on CPOMDPs (Poupart et al., 2015).
- We demonstrate the flexibility of the LP-based approaches by incorporating deterministic policy constraints, and investigating the impact of these constraints on CPOMDP rewards and run times for both finite and infinite horizons problems. Our analysis reveals the feasibility of producing deterministic policies, and also outlines their impact on collected rewards using a direct comparison with their randomized counterparts.

The rest of the paper is organized as follows. We review the relevant literature in Section 2. We provide mathematical description of CPOMDPs and the proposed solution methods for finite and infinite horizon CPOMDP problems in Sections 3 and 4, respectively. Section 5 contains the descriptions and results of our numerical experiments with the CPOMDP problem instances. Section 6 concludes the paper with a summary of our findings and a discussion on future work.

## 2 Literature Review

In this section, we provide an overview of MDPs, POMDPs and CPOMDPs, and review the recent advances on these methodologies. We refer the reader to Puterman (2014) for the technical foundations of MDPs, and Spaan (2012) for a thorough overview of POMDPs.

We can solve MDP models to obtain a policy that specifies a decision rule corresponding to a probability distribution over the action space for all the states and decision epochs (Cassandra, 1994). We typically solve Bellman optimality equations to obtain such policies by using value iteration, policy iteration, or linear programming (Puterman, 2014). Alagoz et al. (2015) empirically demonstrated that linear programming can be used to optimally solve many MDPs significantly faster than standard dynamic programming methods, such as value iteration and policy iteration, while also requiring less memory, and also allowing for problems with a higher number of states to be solved to optimality.

In recent studies, MDPs have been used to model many real-world problems that involve excessively large state and action spaces. Reinforcement learning (RL) has emerged as an effective approach for such problems, and model-free methods (i.e., techniques that do not require a full description of MDP model components) such as Q-learning and deep Q-networks have been shown to achieve state-of-the-art performance as approximation methods (Sutton and Barto, 2018). Some other

studies focused on developing exact solution methods for novel MDP models that are designed for complex problems. For instance, in some domains there exist multiple perspectives on the same phenomenon, resulting in distinct datasets for the same problem. These problems can be better explained by using multiple models simultaneously rather than a single model. Multi-model MDPs were proposed as a novel framework to solve such problems as they allow generating an optimal policy based on the weights assigned to each model (Steimle et al., 2021b). Solving multi-model MDPs typically involves mixed-integer LP formulations. Accordingly, recent studies on multi-model MDPs focused on mathematical optimization techniques such as branch-and-cut and policy-based branch-and-bound methods to improve the solvability of the MDP models (Steimle et al., 2021a; Ahluwalia et al., 2021). While the standard MDP models only involve a generic reward component, it is also possible to have certain costs associated with the actions and states in the decision process. Many real-world problems include a trade-off between available resources and expected reward. Constrained MDPs can be used to incorporate budget considerations into the decision process by employing a cost function which specifies the amount of resources required to take a particular action. There are several approaches in the literature that extend MDP models to handle costs as a separate entity. One approach is to develop customized linear programs that have constraints specifically designed to address any number of cost functions. This approach was employed by McLay and Mayorga (2013) in an infinite horizon setting for the ambulance dispatch problem. Ayvaci et al. (2012b) formulated a constrained MDP model for the finite-horizon breast cancer biopsy decision making problem. They used linear programming to solve their constrained MDP model at varying budget levels to capture the impact of limited resources on the resulting policies that prescribe when to recommend a patient for biopsy.

POMDP models relax the completely observable system state assumption in MDPs. As such, the actions and the policies in POMDPs are determined based on the probability of being in a particular state. Hence, the values are only calculated for belief states, which are defined as a probability distribution over the core state space. POMDPs are important modeling tools for complex problems for which actions can help guiding the system trajectory in a desired manner and gathering information for future decisions. POMDPs have applications in many domains including machine maintenance and replacement (Maillart, 2006), inventory control (Treharne and Sox, 2002) and cancer screening (Ayer et al., 2012; Erenay et al., 2014).

Continuous state space representation and additional model parameters (e.g., observations) further complicate the search for the optimal policy. Sondik (1971) showed that optimal POMDP value functions are piece-wise linear and convex, and can be written as a dot product of belief states and  $\alpha$ -vectors that represent the values at each state. This representation facilitated various exact solution methods such as Monahan’s exhaustive enumeration algorithm (Monahan, 1982) and the Incremental Pruning algorithm (Cassandra, 1998). However, these exact solution methods can typically solve only small problem instances with few core states and actions. Accordingly, most POMDP solution approaches rely on approximation mechanisms. Grid-based approximations are among the most commonly used methods, and can be used to reduce a POMDP to an MDP (Sandikci, 2010). Lovejoy (1991a) showed how to use grid-based approximations to generate lower bounds and upper bounds on the optimal values obtained by the POMDPs. In

a recent study, Kavaklioglu and Cevik (2022) compared distributed, parallel and sequential implementations of Lovejoy (1991a)’s lower bound and upper bound methods.

Many approximation methods for POMDPs with large state spaces focus on point-wise evaluation of the value functions over a set of grid points that corresponds to specific belief states. However, using a fixed set of grid points often fails to produce high quality approximations, especially when the identified grid set cannot adequately describe the belief space. Pineau et al. (2006)’s point-based value iteration algorithm proposes exploration of the value function only at selected belief points. New belief points are considered depending on the updates performed on the selected belief points, which determines the transitions between these points. Another popular point-based approach proposed by Silver and Veness (2010) relies on the Monte Carlo tree search (MCTS) algorithm. MCTS only considers sampled transitions rather than all possible transitions, which helps alleviate computational complexity by only considering a simulated subset of the environment. In practice, MCTS methods are able to quickly converge to a good solution. Parallel implementations allow MCTS algorithms to scale up depending on the problem size and requested solution quality. While the MCTS approach has been shown to converge to optimal solutions in theory, by design they fail to generate exact solutions, nor provide any lower/upper bounds on the optimal values. There are several libraries which provide a standardized method of defining POMDP problems and utilize the previously developed solution algorithms to find optimal/approximate policies. For instance, POMDPs.jl (Egorov et al., 2017) provides access to the implementation of Incremental Pruning and MCTS algorithms among others.

Similar to the relationship between MDP and constrained MDP problems, CPOMDPs extend POMDP models with definitions of cost and cost constraints. CPOMDP solution algorithms attempt to maximize the expected reward without exceeding the available budget. Earlier studies for CPOMDPs focused on dynamic programming based approaches, where separate  $\alpha$ -vectors are generated for cost and reward functions to keep track of the rewards and the costs in the decision process (Kim et al., 2011). This approach is computationally expensive as the number of  $\alpha$ -vectors increases exponentially. As a result, the authors also proposed using an approximate point-based method that keeps track of the reward and cost accrued by each belief point. These  $\alpha$ -vectors can be used to calculate the cost values for the generated solutions, which can then be bounded by a constraint to identify policies that respect the constraint requirements.

Another popular approach to solving POMDP problems is to repeatedly solve linear programs that search for optimal actions at each decision epoch. The resulting LP models can also be augmented with additional constraints to ensure adherence to the cost requirements. One such solution approach is the CALP algorithm proposed by Poupart et al. (2015). CALP reduces a POMDP to an MDP by defining a finite set of belief states  $\mathcal{G}$ , where each  $\mathbf{b} \in \mathcal{G}$  acts as a state in the resulting MDP. The MDP is then modeled using an LP with a cost constraint and an associated budget. An alternative approach is to use a column generation approach, where each column of the LP model represents a separate CPOMDP policy (Walraven and Spaan, 2018). In this method, the LP formulation ensures that the generated policies adhere to the model constraints. The CPOMDP version of the MCTS algorithm developed by Lee et al. (2018) shows promising results for

larger core state spaces. This approach searches for policies that satisfy a given cost constraint or produce no result if it fails to identify a policy that satisfy the constraint.

There are several applications of CPOMDPs in healthcare, which involve enforcing problem-specific constraints. Cevik et al. (2018) proposed a finite-horizon CPOMDP model that maximizes a patient’s quality-adjusted life years (QALYs) while limiting the number of mammographies taken in the patient’s lifetime. They used mixed-integer linear programming methods to solve their CPOMDP models. Gan et al. (2019) developed CPOMDP models to investigate personalized treatment strategies for opioid use disorder. They proposed an approximation approach for solving their CPOMDP model based on Cassandra (1998)’s incremental pruning algorithm, which first dualizes the constraints to the value functions (hence creating an unconstrained formulation), then solve the value functions by assuming large  $\epsilon$ -values in their convergence check.

### 3 Finite Horizon CPOMDPs

Discrete-time finite horizon POMDP models aim to maximize expected total rewards over a given decision horizon. We can define a finite horizon unconstrained POMDP as the 7-tuple  $\langle \mathcal{T}, \mathcal{S}, \mathcal{A}, \mathcal{O}, P, Z, R \rangle$  where  $\mathcal{T} = \{1, 2, \dots, T\}$  represents the set of decision epochs,  $\mathcal{S}$  represents the set of states,  $\mathcal{A}$  represents the set of actions, and  $\mathcal{O}$  represents the set of observations. The last three components govern the uncertainty in a POMDP, with  $P$ ,  $Z$ , and  $R$  corresponding to the transition probabilities, observation probabilities, and rewards in the decision process, respectively. Furthermore, we denote the probability of making a transition from state  $i \in \mathcal{S}$  to  $j \in \mathcal{S}$  at time  $t \in \mathcal{T}$  based on the action  $a \in \mathcal{A}$  as  $p_{ij}^{ta}$ . Similarly, we represent the probability of making observation  $o \in \mathcal{O}$  after making a transition to state  $j \in \mathcal{S}$  at time  $t \in \mathcal{T}$  for action  $a \in \mathcal{A}$  as  $z_{jo}^{ta}$ . Lastly, we take the reward accrued for action  $a \in \mathcal{A}$  in state  $i \in \mathcal{S}$  at time  $t \in \mathcal{T}$  as  $w_{ia}^t$ .

Because the system states are not fully observable in a POMDP, we can define a belief state  $\mathbf{b} = [b_0, b_1, \dots, b_{|\mathcal{S}|}]$  to estimate the underlying system state. A belief state is a probability distribution over the state space, with  $b_i$  representing the probability of occupying state  $i \in \mathcal{S}$ . We refer to the set of all belief states as the belief space, which can be represented as  $\mathcal{B}(\mathcal{S}) = \{\mathbf{b} \mid \sum_{i \in \mathcal{S}} b_i = 1, b_i \geq 0, i \in \mathcal{S}\}$ . At decision epoch  $t \in \mathcal{T}$ , after taking action  $a \in \mathcal{A}$  and making observation  $o \in \mathcal{O}$ , the belief state  $\mathbf{b}$  (i.e.,  $\mathbf{b}_t$ ) is updated to  $\mathbf{b}'$  (i.e.,  $\mathbf{b}_{t+1}$ ), where the  $j$ th component of  $\mathbf{b}'$  can be calculated using Bayes’ rule as follows:

$$b'_j = \frac{\sum_{i \in \mathcal{S}} b_i z_{jo}^{ta} p_{ij}^{ta}}{\sum_{i \in \mathcal{S}} \sum_{i' \in \mathcal{S}} b_i z_{jo}^{ta} p_{i'j}^{ta}}$$

#### 3.1 Unconstrained POMDPs

The expected total reward for a given starting belief state  $\mathbf{b}^0$  in a discrete-time finite horizon unconstrained POMDP can be obtained as

$$\max_{\pi \in \Pi} E_{\mathbf{b}^0}^{\pi} \left[ \sum_{t=0}^{T-1} w_t(X_t, Y_t) + w_T(X_T) \right] \quad (1)$$

where  $\Pi$  represents the policy space, and  $X_t$  and  $Y_t$  correspond to state and action values at time  $t \in \mathcal{T}$ , respectively. The optimization problem given in (1) is intractable. As a result, unconstrained POMDPs are typically solved using recursive Bellman optimality equations as follows:

$$V_T^*(\mathbf{b}) = \sum_{i \in \mathcal{S}} b_i R_i, \quad \mathbf{b} \in \mathcal{B}(\mathcal{S})$$

$$V_t^*(\mathbf{b}) = \max_{a \in \mathcal{A}} \{V_t^a(\mathbf{b})\}, \quad t < T, \mathbf{b} \in \mathcal{B}(\mathcal{S})$$

$$V_t^a(\mathbf{b}) = \sum_{i \in \mathcal{S}} b_i w_i^{ta} + \sum_{i \in \mathcal{S}} b_i \left( \sum_{o \in \mathcal{O}} \sum_{j \in \mathcal{S}} z_{jo}^{ta} p_{ij}^{ta} V_{t+1}^*(\mathbf{b}') \right), \quad a \in \mathcal{A}, t < T, \mathbf{b} \in \mathcal{B}(\mathcal{S})$$

Because there are infinitely many belief states, it is not feasible to directly solve these optimality equations that represent the POMDP value functions. Exact solution methods for unconstrained POMDPs such as Monahan's enumeration algorithm and the Incremental Pruning algorithm typically rely on reformulating the value functions by defining  $\alpha$ -vectors such that  $V_t^*(\mathbf{b}) = \max_{\alpha_t \in \Gamma_t} \{\mathbf{b} \cdot \alpha_t\}$ , where  $\Gamma_t$  represents the set of optimal  $\alpha$ -vectors at time  $t$ . However, these exact solution methods can only solve unconstrained POMDPs with a few states to optimality. Accordingly, various approximation mechanisms have been proposed to solve large unconstrained POMDP models. In this study, we mainly focus on grid-based approximations, which serve as the foundation for our constrained POMDP solution algorithm.

### 3.2 Grid-based approximations for POMDPs

The value function  $V_t^*(\mathbf{b})$ ,  $t \in \mathcal{T}$ ,  $\mathbf{b} \in \mathcal{B}(\mathcal{S})$  can be approximated by discretizing  $\mathcal{B}(\mathcal{S})$  into a set of grid points  $\mathcal{G} = \{\mathbf{g}^k \mid k \in \mathcal{K}\}$  where  $\mathcal{K} = \{1, \dots, |\mathcal{G}|\}$  is index set of  $\mathcal{G}$ . Using these grid points, we define the approximate value function,  $\hat{V}_t(\mathbf{b})$ , as follows

$$\hat{V}_t^a(\mathbf{b}) = \sum_{i \in \mathcal{S}} g_i w_i^{ta} + \sum_{i \in \mathcal{S}} g_i \sum_{o \in \mathcal{O}} \sum_{j \in \mathcal{S}} z_{jo}^{ta} p_{ij}^{ta} \sum_{k \in \mathcal{K}} \beta_k \hat{V}_{t+1}(\mathbf{g}^k), \quad \forall \mathbf{b} \in \mathcal{B}(\mathcal{S}), a \in \mathcal{A}$$

where  $\sum_{k \in \mathcal{K}} \beta_k \hat{V}_{t+1}(\mathbf{g}^k) \approx V_{t+1}^*(\mathbf{b}')$ . That is, the value at the updated belief state  $\mathbf{b}'$  is approximated by a convex combination of the grid values.

By simply focusing on the belief states (i.e., grid points) in the grid set  $\mathcal{G}$ , we can achieve a reduction from POMDPs to MDPs (Sandikci, 2010). That is, we can obtain the approximate value functions as

$$\begin{aligned} \hat{V}_t(\mathbf{g}) &= \max_{a \in \mathcal{A}} \left\{ \hat{V}_t^a(\mathbf{g}) \right\}, & t < T, \quad \mathbf{g} \in \mathcal{G} \\ \hat{V}_T(\mathbf{g}) &= \sum_{i \in \mathcal{S}} g_i R_i, & \mathbf{g} \in \mathcal{G} \end{aligned}$$

Lovejoy (1991b) showed that these approximate values obtained over the grid set  $\mathcal{G}$  provide an upper bound on the optimal values, i.e.,  $V_t^*(\mathbf{g}) \leq \hat{V}_t(\mathbf{g})$  for  $\mathbf{g} \in \mathcal{G}$ .

Accordingly, we refer to this method as the upper bound method for unconstrained POMDPs, which we denote as “UB”.

Finding convex combinations that yield better approximate values (closer to  $Q_{t+1}^*(\mathbf{g}')$ ) is important for obtaining tighter bounds, which can be achieved by computing the  $\beta$ -values as a solution to the following LP model (Sandikci, 2010) as follows:

$$\begin{aligned} \min \quad & \sum_{k \in \mathcal{K}} \hat{V}_{t+1}(\mathbf{g}^k) \beta_k && \text{BetaModel}(\mathbf{g}') \\ \text{s.t.} \quad & \sum_{k \in \mathcal{K}} \beta_k \mathbf{g}_i^k = g'_i, \quad i \in \mathcal{S} \\ & \sum_{k \in \mathcal{K}} \beta_k = 1 \\ & \beta_k \geq 0, \quad k \in \mathcal{K} \end{aligned}$$

Because this particular grid-based approximation mechanism provides an upper bound on the optimal value, the minimization objective of the BetaModel ensures tighter bounds. Furthermore, the constraint set of the BetaModel guarantees that the belief state  $\mathbf{g}'$  can be represented using the grid points in the grid set according to the resulting  $\beta$ -values. Note that these  $\beta$ -values can be pre-computed and stored to be used as inputs for different solution methods. Specifically, if in grid  $\mathbf{g}^k$  at time  $t$  the agent takes action  $a$  and observes  $o$ , then  $\beta_{k\ell}^{tao}$  gives the coefficient of  $\mathbf{g}^\ell$  in the convex combination representation of  $(\mathbf{g}^k)'$ , that is,

$$(\mathbf{g}^k)' = \sum_{\ell \in \mathcal{K}} \beta_{k\ell}^{tao} \mathbf{g}^\ell$$

We note that grid-based approximations can also be used with the solution methods that rely on the  $\alpha$ -vector representation of value functions. For instance, Monahan’s exhaustive enumeration algorithm enumerates all of the  $\alpha$ -vectors at each iteration, which are then pruned to the optimal set of  $\alpha$ -vectors by using Eagle’s reduction and a linear programming-based redundancy/dominance check. We can avoid the full enumeration of the  $\alpha$ -vectors by simply generating one  $\alpha$ -vector per grid point in the grid set, and follow the  $\alpha$ -vector pruning steps of the algorithm to reach an  $\alpha$ -vector set that leads to an approximation of the optimal value functions. Lovejoy (1991b) showed that these approximate values obtained over the grid set  $\mathcal{G}$  provide a lower bound on the optimal values, i.e.,  $\hat{V}_t(\mathbf{g}) \leq V_t^*(\mathbf{g})$  for  $\mathbf{g} \in \mathcal{G}$ . Accordingly, we refer to this method as the lower bound method for unconstrained POMDPs, which we denote as “LB”.

### 3.2.1 Constructing the grid set

There are various grid construction techniques employed for approximating POMDP value functions, each with its own set of advantages and disadvantages. A fixed-resolution grid approach samples beliefs at equidistant intervals in each dimension as specified by the resolution parameter  $\rho$  (Sandikci, 2010). The drawback of this approach is that the size of the resulting grid set  $\mathcal{G}$  grows exponentially with the number of states and  $\rho$ . The cardinality of the resulting grid set  $\mathcal{G}$  for this approach can be obtained as  $|\mathcal{G}| = \binom{|\mathcal{S}|+\rho-1}{|\mathcal{S}|-1}$ . Alternatively, a random sampling



strategy can be used to generate a grid set of a desired size (Suresh, 2005). However, this approach makes it difficult to represent different parts of the grid space with equal likelihood. Additionally, a randomly generated grid set may increase the computational overhead associated with generating the  $\beta$ -values for belief states that fall outside the grid set.

In our numerical analysis, we employ a custom grid construction method. Specifically, we generate a grid set via a modified version of the fixed-resolution grid approach in order to obtain a grid set with  $N$  grid points. For each problem instance, we iteratively generate grid sets  $\mathcal{G}_1, \dots, \mathcal{G}_m$  until  $|\mathcal{G}_m| > N$ , where  $\mathcal{G}_\iota$  is obtained by using  $\rho = \iota$ . Then, we draw  $N - |\mathcal{G}_{m-1}|$  grid points at equal intervals from the set of grid points  $\bar{\mathcal{G}} = \mathcal{G}_m \setminus \mathcal{G}_{m-1}$  and add them to  $\mathcal{G}_{m-1}$  to obtain our final grid set.

### 3.2.2 Linear programming model

When a POMDP is reduced to an MDP using a grid-based approximation, we can employ a backward induction mechanism to solve the resulting model. Alternatively, we can formulate LP models to obtain the optimal values/policies for the MDP model (Puterman, 2014). In order to simplify the notation in the LP model, we first characterize the transition probabilities between the grid points as follows:

$$f_{k\ell}^{ta} = \sum_{o \in \mathcal{O}} \sum_{i \in \mathcal{S}} \sum_{j \in \mathcal{S}} \beta_{k\ell}^{tao} g_i^k z_{jo}^{ta} p_{ij}^{ta} \quad (4)$$

That is,  $f_{k\ell}^{ta} \equiv \Pr_t(\mathbf{g}^\ell | \mathbf{g}^k, a)$  corresponds to the probability of transitioning to grid point  $\mathbf{g}^\ell \in \mathcal{G}$  starting from grid point  $\mathbf{g}^k \in \mathcal{G}$  at time  $t$  after taking action  $a$ .

Let  $u_{tk}$  denote the decision variables that correspond to the optimal values for grid point  $\mathbf{g}^k$  at time  $t$ . We formulate the linear programming model to solve our finite-horizon MDP model as follows:

$$\min \sum_{k \in \mathcal{K}} \delta_k u_{0k} \quad (5a)$$

$$\text{s.t. } u_{tk} \geq \sum_{i \in \mathcal{S}} g_i^k w_i^{ta} + \sum_{\ell \in \mathcal{K}} f_{k\ell}^{ta} u_{t+1\ell}, \quad a \in \mathcal{A}, k \in \mathcal{K}, t < T, \quad (5b)$$

$$u_{Tk} = \sum_{i \in \mathcal{S}} g_i^k R_i, \quad k \in \mathcal{K}, \quad (5c)$$

$$u_{tk} \text{ free}, \quad k \in \mathcal{K}, t \leq T. \quad (5d)$$

The objective function along with the constraints in (5b) and (5c) ensure that the values for the grid points are the ones corresponding to the maximizing action. Note that the  $\delta$  parameter specifies the weight assigned to each grid point, with  $\sum_{k \in \mathcal{K}} \delta_k = 1$ . The constraints in (5b) link the values at successive decision epochs, and the constraints in (5c) determine the values at the final decision epoch where there are no decisions involved.

While the LP model provided in (5) can be used to determine the values at each grid point, it does not directly generate the corresponding optimal policy. As also discussed in (Puterman, 2014), the *dual* of this LP model can be employed to obtain the optimal policies for our MDP model. Let  $x_{tka}$  denote the decision

variables that correspond to the *occupancy measures*, which specify the fraction of time  $\mathbf{g}^k$  is visited and action  $a$  is taken at time  $t$ . Similarly,  $x_{T_k}$  can be defined for the final epoch, which does not involve any decisions regarding the actions. The dual LP model is formulated as follows:

$$\max \sum_{t < T} \sum_{a \in \mathcal{A}} \sum_{k \in \mathcal{K}} \sum_{i \in \mathcal{S}} g_i^k w_i^{ta} x_{tka} + \sum_{k \in \mathcal{K}} \sum_{i \in \mathcal{S}} g_i^k R_i x_{Tk} \quad (6a)$$

$$\text{s.t.} \quad \sum_{a \in \mathcal{A}} x_{0ka} = \delta_k, \quad k \in \mathcal{K}, \quad (6b)$$

$$\sum_{a \in \mathcal{A}} x_{tka} - \sum_{a \in \mathcal{A}} \sum_{\ell \in \mathcal{K}} f_{\ell k}^{t-1a} x_{t-1\ell a} = 0, \quad k \in \mathcal{K}, \quad 0 < t < T, \quad (6c)$$

$$x_{Tk} - \sum_{a \in \mathcal{A}} \sum_{\ell \in \mathcal{K}} f_{\ell k}^{T-1a} x_{T-1\ell a} = 0, \quad k \in \mathcal{K}, \quad (6d)$$

$$x_{Tk} \geq 0, \quad x_{tka} \geq 0, \quad a \in \mathcal{A}, \quad k \in \mathcal{K}, \quad t < T. \quad (6e)$$

Similar to (5), the objective function aims to maximize the expected total reward over the decision horizon as a weighted average over the grid points. The constraints in (6b) link the weights at the first decision epoch with the occupancy measures, implying that  $\sum_{a \in \mathcal{A}} \sum_{k \in \mathcal{K}} x_{0ka} = 1$ . The constraints in (6c) and (6d) link the occupancy measures at the successive decision epochs, and the constraints in (6e) state logical conditions on variables.

### 3.3 Finite Horizon Constrained POMDP Formulation

The discrete-time finite horizon CPOMDP model can be formulated as follows:

$$\max_{\pi \in \Pi} E_{\mathbf{b}^0}^{\pi} \left[ \sum_{t=0}^{T-1} w_t(X_t, Y_t) + w_T(X_T) \right] \quad (7a)$$

$$\text{s.t.} \quad E_{\mathbf{b}^0}^{\pi} \left[ \sum_{t=0}^{T-1} c_t(X_t, Y_t) + c_T(X_T) \right] \leq B \quad (7b)$$

That is, we aim to maximize expected total rewards over the decision horizon  $\mathcal{T}$  starting from the belief state  $\mathbf{b}^0$ , while ensuring that the expected total costs incurred do not exceed the budget limit,  $B$ .

Similar to (1), the CPOMDP model provided in (7) is intractable. Accordingly, we extend the LP-based approximations to unconstrained POMDPs to obtain an approximation mechanism for CPOMDPs. Specifically, the dual LP model provided in (6) can be extended as follows:

$$\max \quad (6a)$$

$$\text{s.t.} \quad (6b) - (6e)$$

$$\sum_{t < T} \sum_{k \in \mathcal{K}} \sum_{a \in \mathcal{A}} \sum_{i \in \mathcal{S}} g_i^k c_i^{ta} x_{tka} \leq B \quad (8a)$$

This LP-based formulation also provides opportunities to incorporate many other problem-specific constraints to CPOMDPs. For instance, we can ensure that the resulting policies are deterministic by introducing binary decision variables  $\theta$  to the formulation, and adding the following constraints to (8):

$$\begin{aligned} x_{tka} &\leq \theta_{tka}, & t < T, \quad k \in \mathcal{K}, \quad a \in \mathcal{A}, \\ \sum_{a \in \mathcal{A}} \theta_{tka} &= 1, & t < T, \quad k \in \mathcal{K}, \\ \theta_{tka} &\in \{0, 1\} & t < T, \quad k \in \mathcal{K}, \quad a \in \mathcal{A}. \end{aligned}$$

We can define similar constraints to ensure that the resulting policies are of threshold-type, that is, the policies are defined based on the threshold levels over the belief states (Puterman, 2014). However, designing such threshold-type policies often require domain expertise, and might not be applicable to all the CPOMDP applications. Also note that introducing binary variables to the model leads to a mixed-integer linear programming (MIP) model, which is significantly more difficult to solve than its LP counterpart. Furthermore, the addition of deterministic policy constraints often results in a reduction in the expected total reward. In our analysis, we investigate the impact of these additional constraints both on run time performance and on the value of the resulting policies.

#### 4 Infinite Horizon CPOMDPs

We can describe discrete-time infinite horizon POMDPs similar to finite horizon POMDPs. The most important distinction for infinite horizon POMDPs is that  $T = \infty$ , which implies the transition probabilities, observation probabilities, and rewards are time-invariant. Accordingly, we use the same notation for infinite horizon POMDPs, except that time index  $t$  is excluded from the notation and mathematical formulas. The Bellman optimality equations for infinite horizon POMDPs are as follows:

$$V^a(\mathbf{b}) = \sum_{i \in \mathcal{S}} b_i w_i^a + \lambda \sum_{i \in \mathcal{S}} b_i \left( \sum_{o \in \mathcal{O}} \sum_{j \in \mathcal{S}} z_{jo}^a p_{ij}^a V^*(\mathbf{b}') \right), \quad a \in \mathcal{A}, \quad \mathbf{b} \in \mathcal{B}(\mathcal{S})$$

Note that, unlike in the finite horizon case, we consider a discounting factor parameter  $0 < \lambda < 1$ , which ensures that the value functions converge.

We utilize the same grid-based approximation scheme for the infinite horizon problem to reduce the POMDP model to an MDP model. Accordingly, the infinite horizon counterpart of (7) can be approximated by using the following LP model:

$$\max \sum_{a \in \mathcal{A}} \sum_{k \in \mathcal{K}} \sum_{i \in \mathcal{S}} g_i^k w_i^a x_{ka} \quad (10a)$$

$$\text{s.t.} \quad \sum_{a \in \mathcal{A}} x_{ka} - \lambda \sum_{a \in \mathcal{A}} \sum_{\ell \in \mathcal{K}} f_{\ell k}^a x_{\ell a} = \delta_k \quad k \in \mathcal{K} \quad (10b)$$

$$\sum_{k \in \mathcal{K}} \sum_{a \in \mathcal{A}} \sum_{i \in \mathcal{S}} g_i^k c_i^a x_{ka} \leq B \quad (10c)$$

$$x_{ka} \geq 0 \quad a \in \mathcal{A}, k \in \mathcal{K} \quad (10d)$$

In (10), the decision variables,  $x_{ka}$ , are the occupancy measures for grid point-action pairs. These variables correspond to the fraction of time  $g^k \in \mathcal{G}$  is visited and action  $a \in \mathcal{A}$  is taken in the long run. Note that the transition probabilities between the grid points  $f_{\ell k}^a$  can be obtained similar to (4). Time-invariant beta values for this calculation can be pre-calculated by using a value iteration algorithm over the grid-based approximation for the unconstrained POMDP model. Specifically, the beta values  $\beta_{k\ell}^{a_o}$  calculated in the last iteration of the value iteration algorithm can be used to obtain  $f_{\ell k}^a$  values.

## 5 Numerical Experiments

In this section, we detail the results from our numerical analysis. We first summarize the experimental setup along with the problem instances. Then, we examine the performance of grid-based approximations for unconstrained POMDPs. Lastly, we discuss the performance of our proposed CPOMDP solution algorithm: iterative transition-based linear programming (ITLP). In our analysis, we compare the performance of ITLP in an infinite horizon setting with Poupart et al. (2015)’s CALP algorithm.

### 5.1 Experimental setup

In this work, we experimented with the five different popular POMDP problem instances listed in Table 1. We extended the problem definitions with a budget constraint and costs to test our algorithm. We briefly describe the problem instances and the parameters below.

Table 1: Specifications of the POMDP problem instances

	$ \mathcal{S} $	$ \mathcal{A} $	$ \mathcal{O} $
tiger (Cassandra et al., 1994)	2	3	2
mcc (Cassandra, 2003)	4	3	3
paint (Cassandra, 2003)	4	4	2
query (Cassandra, 2003)	9	2	3
$4 \times 3$ (Parr and Russell, 1995)	11	4	6

- *tiger*: In this problem, the agent is placed in front of two doors. One door has a tiger behind it and incurs a large negative reward if it is opened, while the other leads to a large positive reward. The problem encodes this information with the two states: `tiger_left` and `tiger_right`. Three actions are available to the agent: `listen`, `open_left` and `open_right`. The `listen` action incurs a reward of  $-1$  and leads to an observation of either `tiger_left` or `tiger_right`, which can be used to reduce the uncertainty in the belief state. Opening the doors with and without

the tiger behind them leads to rewards of  $-100$  and  $+10$ , respectively. Note that the listen action helps reduce uncertainty in the belief state by observing with relatively high accuracy if there is a tiger behind each door. On average, it is logical to listen until the belief state is clearly biased towards one of the doors (i.e., indicating the tiger's location). Accordingly, in the constrained model, we impose restrictions on the number of listen actions that the agent can take before it chooses to open one of the doors. Specifically, we assume a cost of 2 for the listen action and a cost of 1 for the two door opening actions. We then choose a budget which adequately restricts the agent's decisions. For instance, in a finite horizon problem with  $T = 5$  (i.e., four decision epochs), the agent can take at most 1 listen action when  $B = 5$ .

- *paint*: The paint problem involves a part painting task, where a factory automation system aims to ship unblemished and unflawed items while rejecting blemished and flawed ones. There are four states that contain aggregate information about the environment: NFL-NBL-NPA, NFL-NBL-PA, FL-NBL-PA, FL-BL-NPA, where FL/NFL is flawed/unflawed, BL/NBL is blemished/unblemished, PA/NPA is painted/unpainted. Given a part, the automation system can choose to paint, inspect, ship, or reject. If the system ships an unblemished, unflawed, painted part, which corresponds to state NFL-NBL-PA, it receives a reward of  $+1$ ; in any other state, the ship action incurs a reward of  $-1$ . The system also receives a reward of  $+1$  if it rejects a flawed, blemished, unpainted part; similar to the ship action, this action incurs a negative reward of  $-1$  if the part is in any other state. The paint and inspect actions yield no reward regardless of the state that they are taken in. Similar to the tiger model, the inspect action can be used to reduce uncertainty in the belief state. Accordingly, we limit the number of inspect actions by setting the cost of inspecting to 2, while the other actions incur a cost of 1.
- *mcc*: The mcc problem involves an e-commerce website that aims to show suitable ads to target customers. Customers looking to purchase a product can be categorized into one of two states: customers who prefer group 1 items (S1) or customers who prefer group 2 items (S2). Additionally, a customer may be in the process of completing a purchase (SB) or exiting the website (SX). The system can take the following actions: show items from group 1 (A1), show items from group 2 (A2), or show a random mix of items (AN). Showing items from the wrong group increases the risk that a customer will leave the website, while showing the correct items increases the probability of a purchase. Observations O1 and O2, received after each action, indicate that the user is in S1 or S2, respectively. An observation of OX indicates that the user has left the website (i.e., transition to state SX). If the user buys a product from the website (i.e., reaches state SB), the a reward of  $+1$  is collected. In this problem, showing a mix of items (i.e., action AN) can be seen as a last resort when the underlying belief state does not favor a particular core state. In this regard, it can be treated as an exploration action similar to the inspect/listen action in the previous two problems. Accordingly, we impose limits on this exploration action by setting the cost of AN to 20 and the costs for all other actions to 10.
- *query*: The query problem involves a query system with two servers using an aggregate state definition. Each server state can be described as unloaded,

loaded, or down. In total, there are nine states for a two-server system. The agent can query one of the servers (i.e., there are two actions) to learn about its state. The query action leads to one of three observations: no-response, slow-response, and fast-response. The rewards are also linked to the observations, with a reward of 0 for no-response, a reward of 3 for slow-response, and a reward of 10 for fast-response. Unlike the previous problems, the query POMDP formulation does not have an exploration action. For the purposes of imposing budgetary limitations, we assume that querying the first server is more expensive than querying the second, either through bandwidth costs, subscription fees, or some other means. As such, we assign a cost of 2 and 1 for the query actions for servers 1 and 2, respectively.

- $4 \times 3$ : The  $4 \times 3$  maze problem uses the grid world with 11 cells to model an agent trying to reach a designated positive-cell in the grid, while avoiding a specific negative-cell. In order to move between the cells, the agent can take one of the four actions: north, south, east, and west. The observations correspond to the number of walls that the agent observes for the current cell that it occupies. Moreover, the agent can detect the positive-cell and the negative-cell once it occupies those cells. When the positive-cell is reached, a reward of +1 is collected, whereas reaching the negative-cell leads to a reward of -1. Transitioning to any other cells (i.e., states) incurs a small negative reward of -0.04. In our CPOMDP formulation of the  $4 \times 3$  maze problem, we set the cost of taking an action in a single designated cell to 1, and in all other cells to 0. The agent must then navigate the maze while limiting the number of times it passes through this particular cell. Notice that, unlike in the previous CPOMDP formulations, the cost of taking an action in the  $4 \times 3$  problem is state dependent.

Tables 2a and 2b show the allocated budgets for the five CPOMDP problem instances in both their finite horizon and infinite horizon formulations. Table 2a also shows the decision horizon  $T$  for each problem instance. In the finite horizon case, since query and  $4 \times 3$  are larger problem instances that are more difficult to solve, we set their horizon to  $T = 5$  whereas all the other problems are solved for  $T = 20$ . We consider three budget levels: small, medium and large. These budgets help us to examine how the CPOMDP algorithm responds to varying cost constraints. Each selected budget allows for feasible policies to exist, and was selected to adequately constrain the model.

Table 2: CPOMDP budget limits for each problem instance

(a) Finite horizon				(b) Infinite horizon			
Problem	small	medium	large	Problem	small	medium	large
tiger ( $T = 20$ )	21.00	25.00	50.00	tiger	11.50	14.00	22.00
paint ( $T = 20$ )	19.50	22.00	50.00	paint	10.50	12.00	18.00
mcc ( $T = 20$ )	118.00	123.00	140.00	mcc	63.70	66.00	75.00
query ( $T = 5$ )	4.16	4.47	7.00	query	10.32	11.58	16.00
$4 \times 3$ ( $T = 5$ )	0.17	0.25	0.60	$4 \times 3$	0.40	0.45	2.00

With the exception of the  $4 \times 3$  problem, we consider initial (target) belief states  $\mathbf{b}^0$  to be a uniform distribution over the states. For example, the initial belief state for the paint problem is  $\mathbf{b}^0 = [0.25, 0.25, 0.25, 0.25]$ . For the  $4 \times 3$  problem, the uniform distribution is specified over all of the states except for the positive and negative cells that represent terminal states, where the initial probability is zero. We use a discount factor ( $\lambda$ ) of 1.0 for finite horizon problems, and 0.9 for infinite horizon problems. All the experiments are run on a PC with an i7-8700K processor and 32GB of RAM. Implementations are done in python, and the LP models are solved using Gurobi 9.0.

## 5.2 Performance of the grid-based approximations

We first investigate the efficiency and efficacy of the UB approximation method for unconstrained POMDPs as our CPOMDP solution approach is built on this method. In particular, we provide an overview of the computational performance of the LB and UB methods by calculating the optimality gaps, and we demonstrate the need for approximation algorithms by identifying two instances in our set of toy problems where exact solution algorithms are intractable.

The summary results provided in Table 3 provide a comparison of the LB, UB, and Incremental Pruning methods. We first evaluate the values  $V(\mathbf{b}^0)$  at each model’s respective starting belief ( $\mathbf{b}^0$ ). We then investigate the performance of the approximations over the remainder of the belief space by constructing an evaluation grid set  $\bar{\mathcal{G}}$  of size 100, and calculating the LB–UB gap for each  $\mathbf{b} \in \bar{\mathcal{G}}$  as:

$$\text{Gap} = 100 \times \frac{\hat{V}_{\text{UB}}(\mathbf{b}) - \hat{V}_{\text{LB}}(\mathbf{b})}{\hat{V}_{\text{LB}}(\mathbf{b})}$$

The evaluation grid set  $\bar{\mathcal{G}}$  is constructed by randomly sampling belief states, as described by Suresh (2005).

The LB approximation algorithm estimates  $V(\mathbf{b}^0)$  (i.e., the value for the starting belief state) exceptionally well for all five POMDP problem instances, while UB approximation quality deteriorates as the number of states increases, particularly for the finite horizon problems. We observe similar results in our gap calculations, where once again the solution quality deteriorates significantly for finite horizon problems with larger state spaces. We take the query problem as a representative problem instance to investigate the impact of grid set size. We observe modest improvements when increasing the number of grid points for both the finite and infinite horizon problems, at the expense of a significant increase in computation time. Lastly, we find that the Incremental Pruning algorithm is unable to solve the infinite horizon  $4 \times 3$  and query problems within a four hour time limit, while the approximation algorithms can solve the problem in a relatively short amount of time. This shows that even for problems with a few core states, approximation mechanisms are often needed to solve the unconstrained POMDP models.

## 5.3 Analysis with CPOMDP methods

Our CPOMDP solution algorithm, ITLP, allows specifying a probability distribution  $\delta$  over  $\mathbf{g} \in \mathcal{G}$ . Accordingly, the corresponding expected reward and expected

Table 3: Summary results for unconstrained POMDP solution algorithms.

			$V(\mathbf{b}^0)$			CPU (sec.)			Gap (%)			
			LB	IP	UB	LB	IP	UB	min	mean	median	max
T	Problem	$ \mathcal{G} $										
Finite horizon												
20	tiger	200	20.39	20.39	20.39	2.24	57.49	18.53	0.01	0.04	0.01	0.58
	paint	200	3.04	3.04	3.08	2.57	22.73	26.11	1.03	1.48	1.37	3.97
	mcc	200	1.21	1.21	1.22	2.19	8.26	27.46	0.24	0.36	0.34	0.69
5	query	50	18.56	18.56	23.83	2.60	0.62	1.28	21.59	28.17	27.86	40.11
		200	18.56	-	23.70	2.53	-	5.75	21.36	27.36	26.99	39.42
		500	18.56	-	23.53	2.21	-	23.81	21.17	26.47	26.22	38.29
$4 \times 3$		200	0.12	0.12	0.19	1.21	1.87	21.36	0.00	21.77	16.26	145.95
Infinite horizon												
tiger		200	8.51	8.51	8.51	2.14	97.85	96.97	0.01	0.01	0.01	0.06
	paint	200	1.33	1.34	1.34	2.19	30.19	126.13	0.03	0.35	0.06	4.18
	mcc	200	0.69	0.69	0.69	2.60	31.42	81.13	0.07	0.17	0.15	0.63
query		50	48.02	19.02 <sup>†</sup>	48.78	2.77	14400 <sup>†</sup>	10.90	0.92	1.67	1.63	2.91
		200	48.02	-	48.52	8.03	-	68.52	0.56	1.07	1.03	2.30
		500	48.02	-	48.21	37.11	-	336.13	0.20	0.44	0.42	1.00
$4 \times 3$		200	0.75	0.33 <sup>†</sup>	0.84	15.03	14400 <sup>†</sup>	231.18	3.96	10.25	9.89	20.21

IP: Incremental Pruning algorithm

<sup>†</sup> value as of 4 hour timeout<sup>†</sup>  $V(\mathbf{b}^0)$  values are reported for target belief states  $\mathbf{b}^0$ 

cost for such policies depend on both  $\mathcal{G}$  and  $\delta$  as follows:

$$V(\mathcal{G}, \delta) = \sum_{k \in \mathcal{K}} \delta_k V(\mathbf{g}^k), \quad C(\mathcal{G}, \delta) = \sum_{k \in \mathcal{K}} \delta_k C(\mathbf{g}^k)$$

The approximate values of these quantities are denoted by  $\hat{V}(\mathcal{G}, \delta)$  and  $\hat{C}(\mathcal{G}, \delta)$ , and we calculate them using 10,000 simulations where, for each simulation, the initial belief  $\mathbf{b}^0$  is randomly selected using the weights of  $\delta$  corresponding to  $\mathbf{g} \in \mathcal{G}$ . We also report the objective value returned from the linear program denoted by  $\hat{V}_{LP}(\mathcal{G}, \delta)$  and, for a single starting belief  $\mathbf{b}^0$ ,  $\hat{V}_{LP}(\mathcal{G}, \mathbf{b}^0)$ .

For each problem, we generate policies using a grid set  $\mathcal{G}$  of 200 grid points for small, medium, and large budgets, listed in Table 2 for the finite and infinite horizon cases. As was also observed by Poupart et al. (2015), a CPOMDP policy generated by a grid-based approximation does not necessarily adhere to its budget in a general simulation environment. We consider such a policy to be infeasible. In practice, one searches only for feasible policies and discards any policy that exceeds its budget. Poupart et al. (2015) propose performing a binary search for a budget constraint which produces a feasible, near-optimal policy. However, policy generation and evaluation are time consuming processes, which motivates us to minimize the likelihood of producing an infeasible policy in the first place. In the subsequent sections, rather than discarding infeasible policies, we report their  $\hat{V}(\mathcal{G}, \delta)$  and measure the degree to which  $\hat{C}(\mathcal{G}, \delta)$  exceeds the budget limit  $B$  using the following formula:

$$\% \text{-Over} = \begin{cases} 100 \times \frac{\hat{C}(\mathcal{G}, \delta) - B}{B}, & \text{if } \hat{C}(\mathcal{G}, \delta) > B \\ 0, & \text{otherwise} \end{cases} \quad (11)$$



By retaining infeasible policies, we are able to quantify the effect of model complexity and grid size on budget adherence, where Equation (11) provides a measure for the degree to which a policy exceeds its budget.

We note that the process of generating CPOMDP policies using ITLP involves two main steps: (1) generating the transition probabilities (i.e.,  $f_{k\ell}^{ta}$  values), and (2) setting up and solving the final LP given these transition probabilities. We report the elapsed time for each of these steps separately as “cpu-trans” and “cpu-lp”, respectively.

### 5.3.1 Finite horizon CPOMDPs

Table 4 provides the approximate/simulated expected reward  $\hat{V}_{\text{Sim}}(\mathcal{G}, \delta)$  and the %-Over for each model, with an additional column for the simulated expected reward of Incremental Pruning (i.e., for solving the corresponding unconstrained POMDP model). We note that Incremental Pruning results are also dependent on  $\mathcal{G}$  and  $\delta$  as we employ the same simulation mechanism for all cases.

Without access to optimal CPOMDP policies, it is not possible to evaluate the performance of ITLP by considering each budget level individually. Instead, we focus our attention on policy feasibility and the change in  $\hat{V}_{\text{Sim}}(\mathcal{G}, \delta)$  given a change in the budget limits. We observe that for all but the  $4 \times 3$  problem, the generated policies adhere to the budget or exceed it by less than 1%. Table 4 establishes a clear positive relationship between  $B$  and  $\hat{V}_{\text{Sim}}(\mathcal{G}, \delta)$ , with the expected total reward for a large budget policy approaching that of an optimal, unconstrained policy’s reward (IP). Table 4 also provides the run times for each problem, where we observe that for all but the paint problem, the most time consuming step of ITLP is generating the transition probabilities, with the LP taking a smaller (but not insignificant) amount of time.

In addition to providing a comparison of ITLP for varying grid sizes, Figure 1 provides a more granular depiction of how budget adherence and  $\hat{V}_{\text{Sim}}(\mathcal{G}, \delta)$  depend on  $B$  for a representative problem instance, query. Figure 1a shows that  $\hat{V}_{\text{Sim}}(\mathcal{G}, \delta)$  increases with  $B$  until some threshold, at which point further increase in the budget limit does not lead to an increase in  $\hat{V}_{\text{Sim}}(\mathcal{G}, \delta)$ . This behaviour is expected, as increasing the budget corresponds to an increased reward until there is a sufficient budget available to produce an unconstrained policy, at which point the expected reward cannot increase. This is also reflected in the higher budget limits in Figure 1b where, for a sufficiently high budget, %-Over never exceeds zero.

We observe various effects of the grid set size on the quality of the resulting policies. Firstly, we note in Figure 1b that using larger grid sets increases the likelihood of generating a feasible policy. Secondly, we find that increasing the number of grid points does not consistently lead to a lower or higher expected total reward. In particular, in the budget range of 4.00 to 4.63, the model with 200 grid points consistently produces feasible policies that outperform their 500 grid point counterparts. It turns out that the policies obtained with a grid set of size 500 tend to be more conservative with the budget constraint, which allows the model with 200 grid points to produce policies that better utilize the available budget. For larger budgets, we observe that the models with 200 and 500 grid points produce a higher reward than the model with 50 grid points. Lastly, we

Table 4: Finite-horizon CPOMDP results ( $\delta$  is taken as a uniform distribution over the corresponding  $\mathcal{G}$ ).

Problem	$T$	$ \mathcal{G} $		Budget level			IP
				small	medium	large	
tiger	20	200	$\hat{V}_{\text{Sim}}(\mathcal{G}, \delta)$	-650.53	-320.78	28.89	29.10
			$\hat{V}_{\text{LP}}(\mathcal{G}, \delta)$	-604.37	-277.29	22.27	-
			% Over	0.00	0.03	0.00	-
			cpu-trans	19.63	19.63	19.63	-
			cpu-lp	6.15	4.38	5.15	-
paint	20	200	$\hat{V}_{\text{Sim}}(\mathcal{G}, \delta)$	1.00	2.30	3.46	3.69
			$\hat{V}_{\text{LP}}(\mathcal{G}, \delta)$	0.81	2.06	3.41	-
			% Over	0.60	0.77	0.00	-
			cpu-trans	28.32	28.32	28.32	-
			cpu-lp	41.24	26.55	27.17	-
mcc	20	200	$\hat{V}_{\text{Sim}}(\mathcal{G}, \delta)$	0.71	0.93	1.19	1.22
			$\hat{V}_{\text{LP}}(\mathcal{G}, \delta)$	0.70	0.94	1.22	-
			% Over	0.33	0.03	0.00	-
			cpu-trans	31.82	31.82	31.82	-
			cpu-lp	8.67	6.74	6.96	-
query	5	50	$\hat{V}_{\text{Sim}}(\mathcal{G}, \delta)$	21.08	22.10	24.18	24.60
			$\hat{V}_{\text{LP}}(\mathcal{G}, \delta)$	20.77	22.25	24.75	-
			% Over	0.17	0.34	0.00	-
			cpu-trans	0.66	0.66	0.66	-
			cpu-lp	0.46	0.46	0.46	-
		200	$\hat{V}_{\text{Sim}}(\mathcal{G}, \delta)$	20.94	22.10	24.43	24.80
			$\hat{V}_{\text{LP}}(\mathcal{G}, \delta)$	20.88	22.20	24.64	-
			% Over	0.00	0.00	0.00	-
			cpu-trans	5.35	5.35	5.35	-
			cpu-lp	2.36	2.35	2.35	-
		500	$\hat{V}_{\text{Sim}}(\mathcal{G}, \delta)$	20.51	21.58	24.40	24.46
			$\hat{V}_{\text{LP}}(\mathcal{G}, \delta)$	20.52	21.89	24.39	-
			% Over	0.00	0.00	0.00	-
			cpu-trans	27.26	27.26	27.26	-
			cpu-lp	11.96	11.92	11.90	-
$4 \times 3$	5	200	$\hat{V}_{\text{Sim}}(\mathcal{G}, \delta)$	0.13	0.19	0.22	0.27
			$\hat{V}_{\text{LP}}(\mathcal{G}, \delta)$	0.18	0.25	0.28	-
			% Over	17.07	1.98	0.00	-
			cpu-trans	22.38	22.38	22.38	-
			cpu-lp	3.17	3.14	3.14	-

note that the CPU run times increase considerably as we increase the number of grid points from 50 to 500 (see Table 4).

Producing a feasible policy can be a time consuming task. Poupart et al. (2015) suggest performing a binary search over budgets for a feasible policy with an acceptable reward, and Figure 1b suggests that increasing the grid size can also help with generating feasible policies. Both of these processes can add considerable computational overhead and, in the case of increasing grid size, the resulting policy may not fully utilize the available budget. For particularly large problems, increasing the grid size may not be feasible and performing multiple runs may be costly, which motivates choosing a more conservative budget to increase the likelihood of producing a feasible policy in one shot. On the other hand, Figure 1a demonstrates that even small changes to the budget tend to impact  $\hat{V}_{\text{Sim}}(\mathcal{G}, \delta)$ . As a result, a conservative budget choice may result in a considerable decrease in reward.

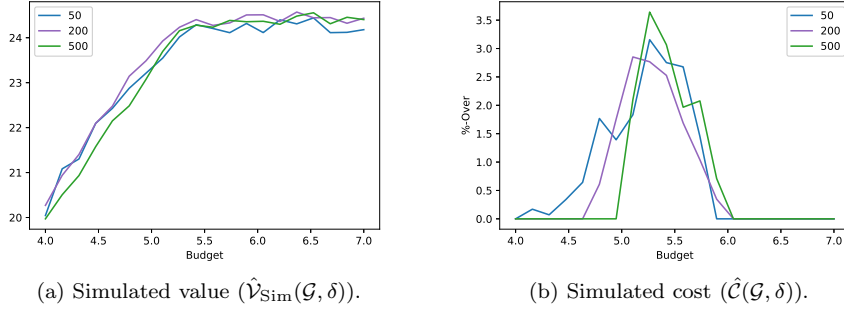


Fig. 1: Detailed finite-horizon CPOMDP results for query problem for different grid set sizes as obtained by simulating the resulting policies.

### 5.3.2 Infinite horizon CPOMDPs

As in the finite horizon case, we use 10,000 simulations to estimate the expected reward and the expected cost, using a horizon of 100 to simulate an infinite horizon. We compare the infinite horizon version of ITLP to Poupart et al. (2015)’s CALP algorithm. CALP policies assume a single starting belief, therefore we specify  $\delta$  as

$$\delta(\mathbf{b}) = \begin{cases} 1, & \text{if } \mathbf{b} = \mathbf{b}^0 \\ 0, & \text{otherwise} \end{cases}$$

Thus,  $\hat{V}(\mathcal{G}, \delta)$  becomes  $\hat{V}(\mathbf{b}^0)$ , and  $\hat{C}(\mathcal{G}, \delta)$  becomes  $\hat{C}(\mathbf{b}^0)$ . Any two policies modeling the same problem and sharing the same grid size use the same  $\mathcal{G}$ . This allows us to directly compare ITLP policies to CALP policies. We compare policies generated using each algorithm for selected small, medium, and large budgets, and compare the  $\hat{V}_{\text{Sim}}(\mathbf{b}^0)$  with the optimal unconstrained  $V(\mathbf{b}^0)$ . Because Incremental Pruning could not generate infinite horizon unconstrained POMDP policies for the  $4 \times 3$  and query problems within the time limit (see Table 3) the reported  $V(\mathbf{b}^0)$  are generated using the LB method for these two problems.

Similar to finite-horizon case, our qualitative analysis focuses on policy feasibility and changes in  $\hat{V}(\mathbf{b}^0)$  with respect to  $B$ . The results in Table 5 show no clear winner between the two algorithms: ITLP performs worse for the simpler toy problems, but performs significantly better for the  $4 \times 3$  problem. For the tiger problem, ITLP produces policies which grossly exceed the budget and show little variation in  $\hat{V}(\mathbf{b}^0)$  between the small and medium budget. In contrast, CALP produces three feasible policies with a significant difference in  $\hat{V}(\mathbf{b}^0)$  between all the budgets. In the paint problem, ITLP produces policies with nearly identical  $\hat{V}(\mathbf{b}^0)$  regardless of the budget, once again grossly exceeding the constraint. CALP performs considerably better, producing a much greater variation in  $\hat{V}(\mathbf{b}^0)$  and exceeding the budget by much less, but still produces infeasible policies for the small and medium budget cases.

CALP performs poorly for the mcc problem, producing policies which all significantly exceed the budget and all yield a nearly identical reward regardless of

Table 5: Infinite horizon CPOMDP results.

Problem	$ \mathcal{G} $		Budget level – ITLP			Budget level – CALP			IP/LB
			small	medium	large	small	medium	large	
tiger	200	$\hat{V}_{\text{Sim}}(\mathbf{b}^0)$	-38.99	-38.88	10.98	-328.96	-131.77	10.75	11.06
		$\hat{V}_{\text{LP}}(\mathbf{b}^0)$	-291.91	-118.46	8.51	-332.02	-135.40	6.13	-
		% Over	28.14	5.26	0.00	0.00	0.00	0.00	-
		cpu-trans	58.99	58.99	58.99	1.21	1.21	1.21	-
		cpu-lp	0.18	0.18	0.18	0.08	0.08	0.08	-
paint	200	$\hat{V}_{\text{Sim}}(\mathbf{b}^0)$	1.58	1.61	1.65	0.05	0.95	1.62	1.69
		$\hat{V}_{\text{LP}}(\mathbf{b}^0)$	0.37	0.88	1.34	0.21	0.83	1.37	-
		% Over	27.32	11.69	0.00	0.77	2.54	0.00	-
		cpu-trans	50.26	50.26	50.26	1.47	1.47	1.47	-
		cpu-lp	0.25	0.24	0.24	0.12	0.12	0.12	-
mcc	200	$\hat{V}_{\text{Sim}}(\mathbf{b}^0)$	0.37	0.52	0.52	0.51	0.52	0.52	0.52
		$\hat{V}_{\text{LP}}(\mathbf{b}^0)$	0.56	0.66	0.69	0.52	0.52	0.52	-
		% Over	4.29	5.25	0.00	20.39	18.14	11.80	-
		cpu-trans	38.64	38.64	38.64	1.67	1.67	1.67	-
		cpu-lp	0.25	0.25	0.25	0.08	0.08	0.08	-
query	50	$\hat{V}_{\text{Sim}}(\mathbf{b}^0)$	34.92	40.02	47.45	33.74	41.98	47.11	49.37
		$\hat{V}_{\text{LP}}(\mathbf{b}^0)$	36.66	42.97	48.75	42.43	45.75	49.11	-
		% Over	0.00	0.01	0.00	0.00	4.71	0.00	-
		cpu-trans	7.83	7.83	7.83	0.31	0.31	0.31	-
		cpu-lp	0.08	0.08	0.08	0.02	0.02	0.02	-
	200	$\hat{V}_{\text{Sim}}(\mathbf{b}^0)$	35.25	41.59	47.94	35.01	42.35	47.91	49.17
		$\hat{V}_{\text{LP}}(\mathbf{b}^0)$	36.55	42.22	48.51	41.52	45.21	48.69	-
		% Over	0.99	3.36	0.00	0.42	5.48	0.00	-
		cpu-trans	81.71	81.71	81.71	1.91	1.91	1.91	-
		cpu-lp	0.41	0.41	0.41	0.15	0.15	0.15	-
	500	$\hat{V}_{\text{Sim}}(\mathbf{b}^0)$	33.94	41.31	48.33	34.18	42.88	48.46	49.22
		$\hat{V}_{\text{LP}}(\mathbf{b}^0)$	36.53	42.24	48.24	41.46	44.98	48.80	-
		% Over	0.00	2.19	0.00	0.00	6.01	0.00	-
		cpu-trans	421.66	421.66	421.66	8.56	8.56	8.56	-
		cpu-lp	1.42	1.39	1.39	2.09	2.08	2.08	-
$4 \times 3$	200	$\hat{V}_{\text{Sim}}(\mathbf{b}^0)$	0.68	0.90	1.14	-0.14	-0.14	-0.13	1.16
		$\hat{V}_{\text{LP}}(\mathbf{b}^0)$	0.39	0.48	0.81	0.24	0.26	0.38	-
		% Over	0.00	2.32	0.00	0.00	0.00	0.00	-
		cpu-trans	155.41	155.41	155.41	9.22	9.22	9.22	-
		cpu-lp	0.32	0.32	0.32	0.13	0.12	0.12	-

budget. ITLP fails to produce feasible policies for the small and medium budget cases, but shows a considerably higher change in  $\hat{V}(\mathbf{b}^0)$  between the small and medium budgets and, in the large budget case, yields a reward identical to the unconstrained optimal policy while coming in under budget. CALP is also able to produce a policy which yields the same reward as an optimal unconstrained policy, but it does so by exceeding the budget by nearly 12%.

Unlike in the finite horizon case, ITLP produces policies for the  $4 \times 3$  problem which perform exceptionally well, only exceeding the medium budget. There is also a significant increase in  $\hat{V}(\mathbf{b}^0)$  with increasing budget. In contrast, CALP only generates excessively conservative policies, all of which are feasible but none of which comes close to  $\hat{V}(\mathbf{b}^0)$  generated by ITLP for the low budget case.

Figure 2 provides a comparison of ITLP and CALP for varying grid sizes for the query problem, which is selected as the representative problem instance. The most notable effect of increasing grid set size for infinite horizon ITLP is that, similar to our finite horizon results, the region of budgets over which ITLP exceeds the

budget constraint generally tends to narrow as the number of grid points increases. In contrast, the region over which CALP policies exceed the budget constraint actually increases slightly with the number of grid points. We observe that for policies which exceed the budget, the policy with the greater value tends to be the one that exceeds the budget with a greater margin. As policies generated by ITLP tend to exceed the budget by less, they also yield moderately lower values.

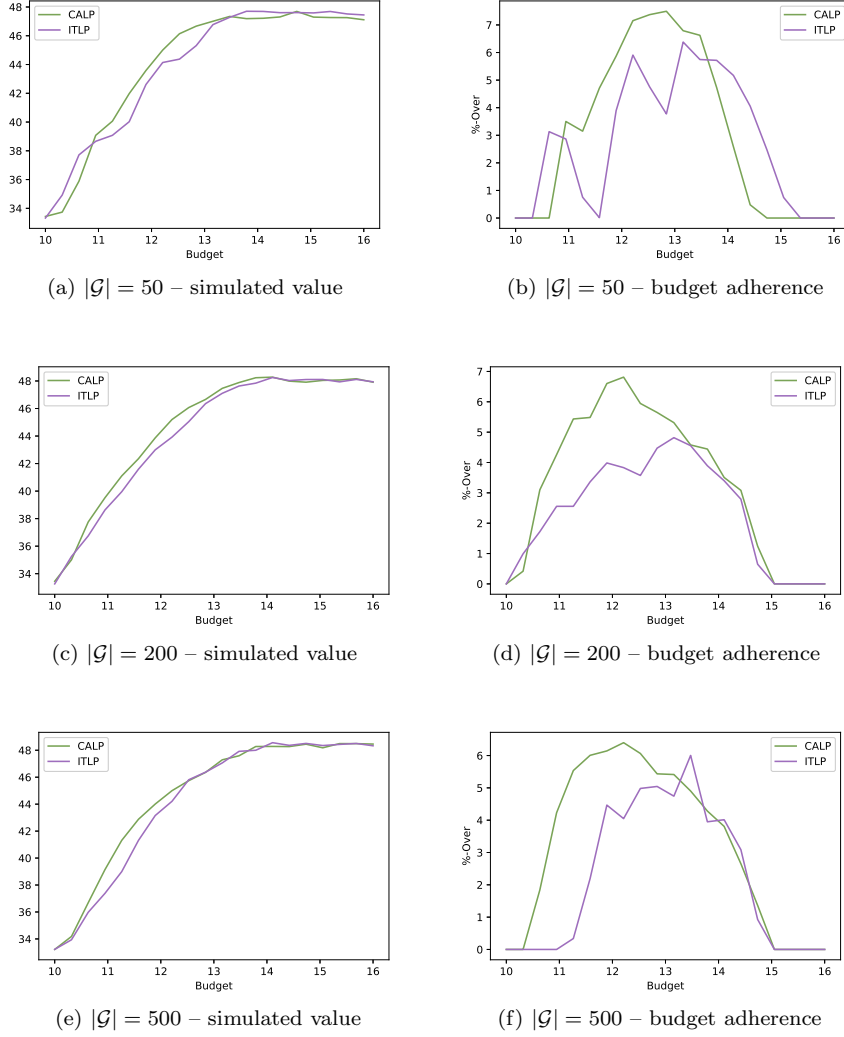


Fig. 2: Comparison of infinite horizon CPOMDP policies for different grid set sizes (budget adherence is given by Equation 11).

We also summarize the query problem results in Table 5, which provides policy generation times for each of these policies. In the finite horizon case, the LP was considerably more complicated, which is reflected in Table 5 as we observe that `cpu-lp` is insignificant in comparison to `cpu-trans`, unlike in Table 4. We observe that ITLP’s iterative approach to generating transition probabilities results in considerably higher run times compared to CALP, with the `cpu-lp` also being slightly longer for the ITLP algorithm in most cases.

#### 5.4 Impact of deterministic policy constraints

When a POMDP is transformed into a CPOMDP by adding a budget constraint, we can no longer assume that an optimal deterministic policy exists (Puterman, 2014; Kim et al., 2011). Despite this, there are still many applications where a suboptimal deterministic policy is preferred to an optimal randomized one, such as in the field of medical diagnosis (Ayvaci et al., 2012a; Cevik et al., 2018). As a result, there is a need to quantify the impact of the deterministic policy constraints on the quality of the resulting policies. As a deterministic policy obtained with this method cannot collect a higher reward than its randomized policy counterpart, we compare the performance of the LP and MIP approaches using “% Difference”, calculated as

$$\% \text{ Difference} = 100 \times \frac{\hat{V}_{LP}(b^0) - \hat{V}_{MIP}(b^0)}{|\hat{V}_{LP}(b^0)|} \quad (12)$$

We consider 100 distinct belief states for each of the three budget levels and report the aggregate % Difference values in figures 3 and 4. In the finite horizon case, we observe that, except for the  $4 \times 3$  problem, there is very little difference between the value attained by policies from LP and MIP models. In contrast, we observe in Figure 4 that a significant number of infinite horizon policies perform substantially worse when subject to deterministic policy constraints.

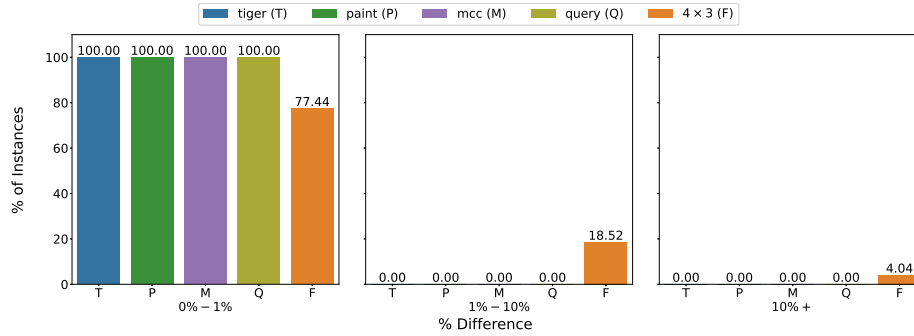


Fig. 3: Finite horizon % Difference between LP and MIP policy values.

We observe that each of the problems with an exploratory action (tiger, paint, mcc) are able to adapt very well to the finite horizon deterministic policy constraints but, as expected, struggle in an infinite horizon setting as they cannot

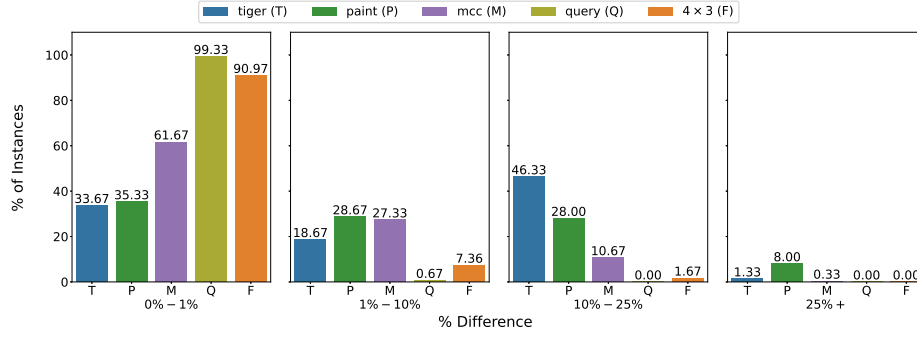


Fig. 4: Infinite horizon % Difference between LP and MIP policy values.

distribute their exploration over the various time steps in an infinite horizon setting. We observe that deterministic policies lead to a smaller value deterioration for the  $4 \times 3$  problem in an infinite horizon setting. This result is somewhat expected: recall that the  $4 \times 3$  agent must traverse a grid to reach the goal state. In the finite horizon case with  $T = 5$ , budget limitations could prevent the agent from following a path that leads to the goal using the available number of actions. This can cause the agent not to collect any rewards in some cases. In the infinite horizon formulation, the agent can simply take a longer path, incurring a small penalty for taking a higher number of decision epochs to reach the goal, but these additional negative rewards are substantially smaller than the impact of not reaching the goal state.

Finally, we investigate the effect of deterministic policy constraints on run time. For this experiment, we make some adjustments to our previous setup to ensure that we observe statistically relevant differences in the run times. For all problems, we consider a finite horizon with  $T = 20$  and  $|\mathcal{G}| = 500$ . We observe the CPU time for 100 distinct budget levels in both the randomized (LP) and deterministic (MIP) cases. The collected run times reflect only the amount of time spent by the LP solver searching for an optimal policy. We allow the solver to search for up to 1,000 seconds before timeout. Note that we also investigated the impact of deterministic policy constraints on infinite horizon problems, and observed that these constraints did not produce a meaningful increase in run time for this case. This result can be attributed to the fact that LP/MIP models are substantially smaller in the case of infinite horizon problem, rendering the impact of additional deterministic policy constraints on run times negligible. However, for larger grid set sizes (e.g., in the order of tens of thousands), we might expect noticeable differences for the infinite horizon problems as well.

Figure 5 compares the run times for the finite horizon LP and MIP problems on a log scale. Surprisingly, the tiger problem is the only case which exceeds the timeout period for the MIP model, with 23 of 100 budgets timing out at 1,000 seconds. Considering each model individually, we observe that the MIP models tend to take considerably longer than their LP counterparts, and they also contribute much more variance to run time. Additionally, we note that MIP models require a timeout period to be specified to ensure that they complete execution in a reasonable amount of time. However, while the run times are considerably

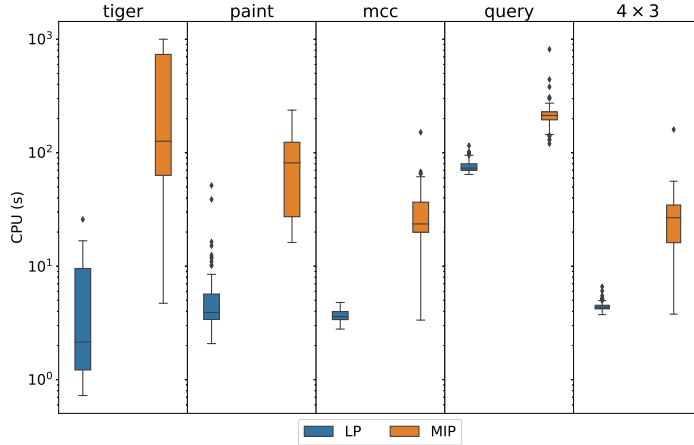


Fig. 5: CPU time for LP versus MIP constrained problems over 100 budgets using a 1,000 second timeout. For each problem,  $T = 20$  and  $|\mathcal{G}| = 500$ .

longer, they are not impractical and, in combination with the results in Figure 3, we conclude that deterministic policies, especially in the finite horizon setting, are viable to produce in a practical environment, and are not always substantially inferior to stochastic policies.

## 6 Conclusion

In this study, we investigated LP-based solution approaches for CPOMDPs. We separately examined finite horizon and infinite horizon CPOMDP problems by adapting five POMDP problem instances from the literature. We established the validity of our approach by first quantifying the performance of the LB and UB POMDP approximation algorithms. We then developed our proposed CPOMDP solution algorithm, ITLP, as an extension of the UB algorithm. We investigated the performance of ITLP for finite horizon problems and observed that, while some policies exceeded the budget constraint, all of them adapted to the constraint. This suggests that, as proposed by Poupart et al. (2015), a post-processing over the generated policies can be adopted to obtain feasible, constrained policies.

In our analysis of ITLP for infinite horizon CPOMDPs, we provided a direct comparison to Poupart et al. (2015)’s CALP algorithm. These algorithms each work by reducing a CPOMDP to a constrained MDP through the use of a grid set. Our results show that while neither algorithm is best suited for all CPOMDP problems, each is able to outperform the other in several problem instances. Consistent with the findings in Poupart et al. (2015), we observed that neither algorithm is guaranteed to produce policies that strictly adhere to the budget constraint. To that extent, we compared the degree to which generated policies exceeded their budget. This allowed for a more accurate comparison of the performance of each algorithm, and offered insights into the various factors which contribute to the budget adherence. In the context of our comparison, the key difference between the algorithms lies in the generation of approximate transition probabilities. CALP



approximates transition probabilities using a single time step, while ITLP iteratively generates transition probabilities until convergence. This iterative process has a negative impact on ITLP’s run time, but we observed for both the  $4 \times 3$  and mcc problems that it allows the algorithm to generate far superior policies in some cases. ITLP further distinguishes itself from CALP by providing a mechanism for solving finite horizon problems, by supporting deterministic policy constraints, and by allowing for a probability distribution to be specified over  $\mathcal{G}$ , as opposed to enforcing that a single grid  $\mathbf{g} \in \mathcal{G}$  be chosen as the initial belief state.

To conclude our experiments, we investigated the performance of deterministic policy constraints on both the expected total rewards and run times for each CPOMDP problem. We observed that, while in theory optimal CPOMDP policies are stochastic, in many contexts and especially in the finite horizon case, the superiority of stochastic policies is negligible. Additionally, we observe that while run times are considerably longer for deterministic policy generation, typical run times are not prohibitively long when the grid set sizes or decision epochs are not excessively large. Together, these results demonstrate that deterministic CPOMDP policies can be a viable solution in many contexts where they might be necessary, while also demonstrating that stochastic policies, although potentially more difficult to implement in practice, are preferred when possible.

While we experimented with five different problem instances, a more extensive empirical analysis can help further validate our findings. We observed that the design of the grid set, particularly its size, helps to increase budget adherence. We also demonstrated that while our LP formulation allows for additional constraints to be incorporated, such additions come at the expense of computational overhead. In such cases, advanced optimization techniques such as column and row generation may help to improve solvability. Lastly, we observed that the occupancy measure values, particularly for finite horizon problems, often took very small values, resulting in numerical stability issues. We leave the investigation of such computational issues to future work.

### Data availability statement

All the datasets are publicly available, and can be obtained using the cited sources.

### Disclosure statement

No potential conflict of interest was reported by the authors.

### References

- Ahluwalia VS, Steimle LN, Denton BT (2021) Policy-based branch-and-bound for infinite-horizon multi-model markov decision processes. *Computers & Operations Research* 126:105108
- Alagoz O, Ayvaci MU, Linderoth JT (2015) Optimally solving markov decision processes with total expected discounted reward function: Linear programming revisited. *Computers & Industrial Engineering* 87:311–316

- Ayer T, Alagoz O, Stout N (2012) A POMDP approach to personalize mammography screening decisions. *Operations Research* 60(5):1019–1034
- Ayvaci M, Alagoz O, Burnside E (2012a) The effect of budgetary restrictions on breast cancer diagnostic decisions. *M&SOM* 14(4):600–617
- Ayvaci MU, Alagoz O, Burnside ES (2012b) The effect of budgetary restrictions on breast cancer diagnostic decisions. *Manufacturing & Service Operations Management* 14(4):600–617
- Bravo RZB, Leiras A, Cyrino Oliveira FL (2019) The use of uav s in humanitarian relief: an application of pomdp-based methodology for finding victims. *Production and Operations Management* 28(2):421–440
- Cassandra A (1994) Optimal policies for partially observable Markov decision processes. Brown University, Providence, RI
- Cassandra A (2003) Simple examples. <http://www.pomdp.org/examples/>, accessed: 2019-09-01
- Cassandra AR (1998) Exact and approximate algorithms for partially observable Markov decision processes. Brown University
- Cassandra AR, Kaelbling LP, Littman ML (1994) Acting optimally in partially observable stochastic domains. In: AAAI, AAAI
- Cevik M, Ayer T, Alagoz O, Sprague BL (2018) Analysis of mammography screening policies under resource constraints. *Production and Operations Management* 27(5):949–972
- Cui Y, Lau VK, Huang H (2013) Dynamic partial cooperative mimo system for delay-sensitive applications with limited backhaul capacity. *IEEE transactions on wireless communications* 12(11):5889–5895
- Egorov M, Sunberg ZN, Balaban E, Wheeler TA, Gupta JK, Kochenderfer MJ (2017) Pomdps. jl: A framework for sequential decision making under uncertainty. *The Journal of Machine Learning Research* 18(1):831–835
- Erenay F, Alagoz O, Said A (2014) Optimizing colonoscopy screening for colorectal cancer prevention and surveillance. *M&SOM* 16(3):381–400
- Gan K, Scheller-Wolf AA, Tayur SR (2019) Personalized treatment for opioid use disorder. Available at SSRN 3389539
- Kavaklioglu C, Cevik M (2022) Scalable grid-based approximation algorithms for partially observable markov decision processes. *Concurrency and Computation: Practice and Experience* 34(5):e6743
- Kim D, Lee J, Kim K, Poupart P (2011) Point-based value iteration for constrained POMDPs. In: Twenty-Second International Joint Conference on Artificial Intelligence, pp 1968–1974
- Lee J, Kim GH, Poupart P, Kim KE (2018) Monte-carlo tree search for constrained pomdps. *Advances in Neural Information Processing Systems* 31
- Lovejoy W (1991a) A Survey of Algorithmic Methods for Partially Observed Markov Decision Processes. *Annals of Operations Research* 28:47–66
- Lovejoy W (1991b) Computationally feasible bounds for partially observed Markov decision processes. *Operations Research* 39(1):162–175
- Maillart LM (2006) Maintenance policies for systems with condition monitoring and obvious failures. *IIE Transactions* 38(6):463–475
- McLay LA, Mayorga ME (2013) A dispatching model for server-to-customer systems that balances efficiency and equity. *Manufacturing & Service Operations Management* 15(2):205–220

- Monahan G (1982) State of the art — A survey of partially observable Markov decision processes: Theory, models, and algorithms. *Management Science* 28(1):1–16
- Pajarinen J, Kyrki V (2017) Robotic manipulation of multiple objects as a pomdp. *Artificial Intelligence* 247:213–228
- Parr R, Russell S (1995) Approximating optimal policies for partially observable stochastic domains. In: *IJCAI, IJCAI*, vol 95, pp 1088–1094
- Pineau J, Gordon G, Thrun S (2006) Anytime Point-Based Approximations for Large POMDPs. *JAIR* 27:335–380
- Poupart P, Malhotra A, Pei P, Kim KE, Goh B, Bowling M (2015) Approximate linear programming for constrained partially observable markov decision processes. In: *Proceedings of the AAAI Conference on Artificial Intelligence*, vol 29
- Puterman ML (2014) *Markov decision processes: discrete stochastic dynamic programming*. John Wiley & Sons
- Sandikci B (2010) Reduction of a pomdp to an mdp. *Wiley Encyclopedia of Operations Research and Management Science*
- Schöpe M, Driessen H, Yarovoy A (2021) A constrained pomdp formulation and algorithmic solution for radar resource management in multi-target tracking. *ISIF Journal of Advances in Information Fusion* 16(1):31
- Silver D, Veness J (2010) Monte-carlo planning in large pomdps. *Advances in neural information processing systems* 23
- Sondik EJ (1971) *The optimal control of partially observable Markov processes*. Stanford University
- Spaan MT (2012) Partially observable markov decision processes. In: *Reinforcement Learning*, Springer, pp 387–414
- Steimle LN, Ahluwalia VS, Kamdar C, Denton BT (2021a) Decomposition methods for solving markov decision processes with multiple models of the parameters. *IIE Transactions* 53(12):1295–1310
- Steimle LN, Kaufman DL, Denton BT (2021b) Multi-model markov decision processes. *IIE Transactions* 53(10):1124–1139
- Suresh (2005) Sampling from the simplex. Available from <http://geomblog.blogspot.com/2005/10/sampling-from-simplex.html> Accessed on February 26, 2015.
- Sutton RS, Barto AG (2018) *Reinforcement learning: An introduction*. MIT press
- Treharne JT, Sox CR (2002) Adaptive inventory control for nonstationary demand and partial information. *Management Science* 48(5):607–624
- Walraven E, Spaan MT (2018) Column generation algorithms for constrained pomdps. *Journal of artificial intelligence research* 62:489–533
- Wang M, Dearden R, Hawes N (2015) Robot plans execution for information gathering tasks with resources constraints. In: *2015 European Conference on Mobile Robots (ECMR)*, IEEE, pp 1–6
- Young S, Gašić M, Thomson B, Williams JD (2013) Pomdp-based statistical spoken dialog systems: A review. *Proceedings of the IEEE* 101(5):1160–1179